

# REDSHIFTS FOR 2410 GALAXIES IN THE CENTURY SURVEY REGION<sup>1,2</sup>

GARY WEGNER AND JOHN R. THORSTENSEN

Department of Physics and Astronomy, 6127 Wilder Laboratory, Dartmouth College, Hanover, NH 03755-3528

MICHAEL J. KURTZ, WARREN R. BROWN, DANIEL G. FABRICANT, MARGARET J. GELLER, AND JOHN P. HUCHRA  
 Harvard-Smithsonian Astrophysical Observatory, 60 Garden Street, Cambridge, MA 02138

RONALD O. MARZKE

Department of Astronomy and Physics, San Francisco State University, 1600 Holloway Avenue, San Francisco, CA 94132

AND

SHOKO SAKAI

Division of Astronomy and Astrophysics, Department of Physics and Astronomy, University of California, Los Angeles, 405 Hilgard Avenue, Los Angeles, CA 90095-1562

Received 2001 June 7; accepted 2001 August 15

## ABSTRACT

The Century Survey strip covers 102 deg<sup>2</sup> within the limits  $8^{\text{h}}5 \leq \alpha \leq 16^{\text{h}}5$ ,  $29^{\circ}0 \leq \delta \leq 30^{\circ}0$ , equinox B1950.0. The strip passes through the Corona Borealis supercluster and the outer region of the Coma cluster. Within the Century Survey region, we have measured 2410 redshifts that constitute four overlapping complete redshift surveys: (1) 1728 galaxies with Kron-Cousins  $R_{\text{ph}} \leq 16.13$  covering the entire strip, (2) 507 galaxies with  $R_{\text{ph}} \leq 16.4$  in right ascension range  $8^{\text{h}}32^{\text{m}} \leq \alpha \leq 10^{\text{h}}45^{\text{m}}$ , equinox B1950.0, (3) 1251 galaxies with absorption- and  $K$ -corrected  $R_{\text{CCDc}} \leq 16.2$  (where “c” indicates “corrected”) covering the right ascension range  $8^{\text{h}}5 \leq \alpha \leq 13^{\text{h}}5$ , equinox B1950.0, and (4) 1255 galaxies with absorption- and  $K$ -corrected  $V_{\text{CCDc}} \leq 16.7$  also covering the right ascension range  $8^{\text{h}}5 \leq \alpha \leq 13^{\text{h}}5$ , equinox B1950.0. All these redshift samples are more than 98% complete to the specified magnitude limit. We derived samples 1 and 2 from scans of the POSS1 red (E) plates calibrated with CCD photometry. We derived samples 3 and 4 from deep  $V$  and  $R$  CCD images covering the entire region. We include coarse morphological types for all the galaxies in sample 1. The distribution of  $(V-R)_{\text{CCD}}$  for each type corresponds appropriately with the classification.

**Key words:** cosmology: observations — cosmology: theory — galaxies: distances and redshifts — large-scale structure of universe

**On-line material:** machine-readable tables

## 1. INTRODUCTION

Redshift surveys have come of age. A host of samples derived from optical imaging surveys cover sizable solid angles and contain more than 1000 galaxies (Davis et al. 1982; Geller & Huchra 1989; Giovanelli & Haynes 1989; Loveday et al. 1992; da Costa et al. 1994; Ratcliffe et al. 1996; Shectman et al. 1996; Vettolani et al. 1997; York et al. 2000; Cross et al. 2001). The surveys range from recent megaprojects such as the 2dF (Cross et al. 2001) and Sloan (York et al. 2000) surveys to the smaller ESO Key Program (Vettolani et al. 1997) and the Century Surveys, which we are discussing here (Geller et al. 1997). Only three of these surveys are in the  $R$ -band: the Las Campanas (Shectman et al. 1996), Sloan (York et al. 2000), and Century (Geller et al. 1997) surveys.

We acquired the 2410 redshifts in this paper to complete four redshift surveys in the Century Survey strip: (1) the original Century Survey of 1728 galaxies Kron-Cousins (Kron, White, & Gascoigne 1953)  $R_{\text{ph}} \leq 16.13$  covering the entire strip (Geller et al. 1997, hereafter OCS), (2) a survey including 508 galaxies with  $R_{\text{ph}} \leq 16.4$  in the right ascen-

sion range  $8^{\text{h}}32^{\text{m}} \leq \alpha \leq 10^{\text{h}}45^{\text{m}}$ , equinox B1950.0 (hereafter DCS), (3) a survey of 1251 galaxies with absorption- and  $K$ -corrected  $R_{\text{CCDc}} \leq 16.2$  covering the right ascension range  $8^{\text{h}}5 \leq \alpha \leq 13^{\text{h}}5$ , equinox B1950.0 (Brown et al. 2001, hereafter RCS), and (4) a survey of 1255 galaxies with absorption- and  $K$ -corrected  $V_{\text{CCDc}} \leq 16.7$  also covering the right ascension range  $8^{\text{h}}5 \leq \alpha \leq 13^{\text{h}}5$ , equinox B1950.0 (Brown et al. 2001, hereafter VCS). All these sets of redshifts are more than 98% complete to the specified magnitude limit.

The OCS cuts through the Great Wall and provides a sample of galaxies 2.3 mag fainter than the characteristic  $L_*$  magnitude within it. The redshift survey also includes the Corona Borealis supercluster ( $\alpha = 15^{\text{h}}3$  to  $15^{\text{h}}6$ ,  $\delta = 27^{\circ}5$  to  $32^{\circ}$ , equinox B1950.0) containing the galaxy cluster A2079 and the outer fringes of A1656, the Coma cluster ( $\alpha = 12^{\text{h}}57^{\text{m}}5$ ,  $\delta = 28^{\circ}15'$ , equinox B1950.0). In addition, the survey samples the Abell galaxy clusters A690, A1185, A1213, A2162, and A2175.

We include the photographic magnitudes,  $R_{\text{ph}}$ , used to define the OCS and DCS samples. For the galaxies in the OCS, we list morphological types. To our knowledge, there are no other complete redshift surveys to this depth with morphological types.

Section 2 discusses the photographic photometry. We use the CCD photometry for the RCS and VCS (Brown et al. 2001) to examine residual systematics in the photographic photometry. We also use the CCD photometry to show that

<sup>1</sup> Work reported here is based partly on observations obtained at the Michigan-Dartmouth-MIT Observatory.

<sup>2</sup> Work reported here is based partly on observations at the Multiple Mirror Telescope, a joint facility of the Smithsonian Institution and the University of Arizona.

the morphological types are sensible. Section 3 describes the spectroscopic observations and data reduction procedures. Section 4 gives the catalog of redshifts, photographic magnitudes, and morphological types, along with a brief discussion of the OCS and DCS samples derived from the photographic photometry. We conclude in § 5.

## 2. PHOTOMETRIC DATA AND SAMPLE SELECTION

We constructed the OCS galaxy catalog from scans of the POSS1 E plates according to the procedures outlined by Kurtz et al. (1985). For each galaxy in the catalog, we derived an isophotal magnitude to a bright limiting isophote, which varies unavoidably from plate to plate. Two drift scans from  $8^{\text{h}}27^{\text{m}}$  to  $11^{\text{h}}55^{\text{m}}55^{\text{s}}$  and from  $11^{\text{h}}50^{\text{m}}$  to  $15^{\text{h}}45^{\text{m}}$  provided the basis for the magnitude calibration (Ramella, Nonino, & Geller 1995; Kent, Ramella, & Nonino 1993). The drift scans are both centered at  $\delta = 29^{\circ}5$ . The drift scan for early  $\alpha$  values was done with the 1.2 m telescope and for late  $\alpha$  values with the 61 cm telescope (now retired) of F. L. Whipple Observatory (FLWO). We also used pointed observations to check the drift scans and to calibrate the three POSS plates E924, E1365, and E134, which cover the right ascension ranges  $8^{\text{h}}32^{\text{m}}32^{\text{s}}$  to  $8^{\text{h}}58^{\text{m}}50^{\text{s}}$  and  $15^{\text{h}}53^{\text{m}}$  to  $16^{\text{h}}19^{\text{m}}44^{\text{s}}$ .

We used an iterative procedure to calibrate the photographic photometry. First, we fixed a preliminary zero point on each plate by comparing the instrumental magnitudes with the drift scans of Ramella et al. (1995) and Kent et al. (1993) at  $R = 16.0$ . We then combined data from all plates and obtained a preliminary global slope for the scale error. We then redetermined the zero point (at  $R = 16.0$ ) for each plate and fitted a new global slope. The procedure converged after two iterations.

Recently Brown et al. (2001) obtained  $V$  and  $R_{\text{KC}}$  photometry for 1295 galaxies in the Century strip from CCD images with median rms errors of  $\pm 0.042$  mag in both  $R_{\text{CCD}}$  and  $V_{\text{CCD}}$ . By comparing the galaxy coordinates from the CCD data with those from the PDS scans of the POSS1 plates, we estimate the rms error in the photographic coordinates,  $\Delta\theta = \pm 0''.29$ .

The extensive CCD photometry enables a clean evaluation of the rms error in the photographic magnitudes and of the residual systematic errors. Figure 1 compares the photographic Century Survey (CS) photometry with the CCD photometry of Brown et al. (2001). The zero-point offset,  $\Delta = R_{\text{CCD}} - R_{\text{ph}} = 0.014 \pm 0.22$ , is well within the average zero-point error in the CCD photometry ( $\pm 0.034$  mag). The  $\pm 0.22$  mag scatter of the photographic relative to the CCD photometry is consistent with the  $\pm 0.25$  mag photographic scatter estimated by Geller et al. (1997).

Figure 2 shows  $\Delta$  as a function of  $R_{\text{CCD}}$  for 935 CS galaxies. The comparison indicates a residual slope of  $0.07 \text{ mag mag}^{-1}$ , a 10% error in the original zero-point slope. The brightest  $R < 11$  CS galaxies are  $\sim 0.5$  mag brighter than the photographic magnitude; the offset decreases for fainter galaxies. This error is consistent with variation in the non-linearity from plate to plate.

Figure 3 shows  $\Delta$  as a function of the peak  $R$  surface brightness returned by SExtractor (Bertin & Arnouts 1996) from the CCD data for 429 galaxies with  $15.5 \leq R_{\text{CCD}} \leq 16.13$ . In this apparent magnitude range, the zero-point offset between the photographic and CCD magnitudes is small. The sample of galaxies in Figure 3 have a cleanly defined surface brightness peak (i.e., there are no cosmic

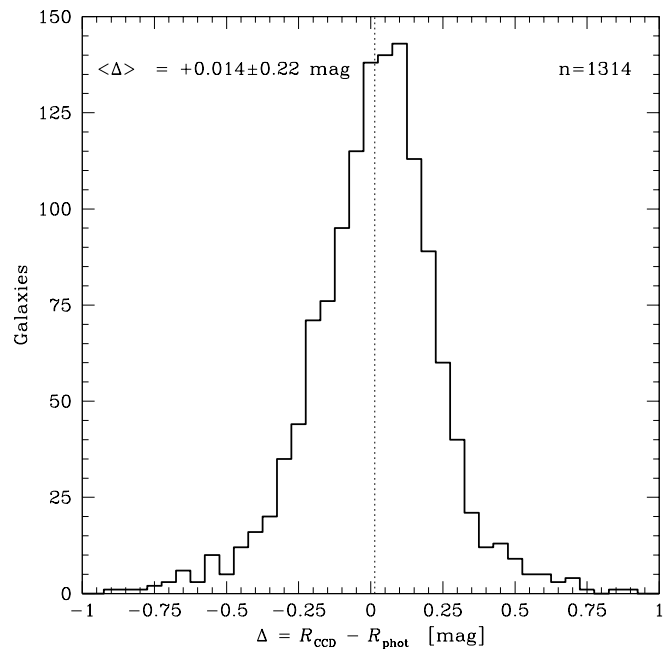


FIG. 1.—Histogram of  $\Delta = R_{\text{CCD}} - R_{\text{ph}}$ . The dotted line shows the zero-point offset,  $\Delta = 0.014$  mag. The dispersion is  $\pm 0.22$  mag, comparable with the  $\pm 0.25$  mag error in  $R_{\text{ph}}$  originally estimated by Geller et al. (1997).

rays or bad columns, no superposed stars, etc.). For the lowest surface brightness galaxies, the photographic magnitudes are brighter than the CCD magnitudes; for high surface brightness galaxies, the effect is the reverse. The sense of the systematic deviations is as expected from the effect of saturation on the photographic magnitudes. The dashed line in Figure 3 shows the best-fit relation  $\Delta = 0.13\mu_R - 2.59$ , where  $\mu_R$  is the peak  $R$ -band surface brightness.

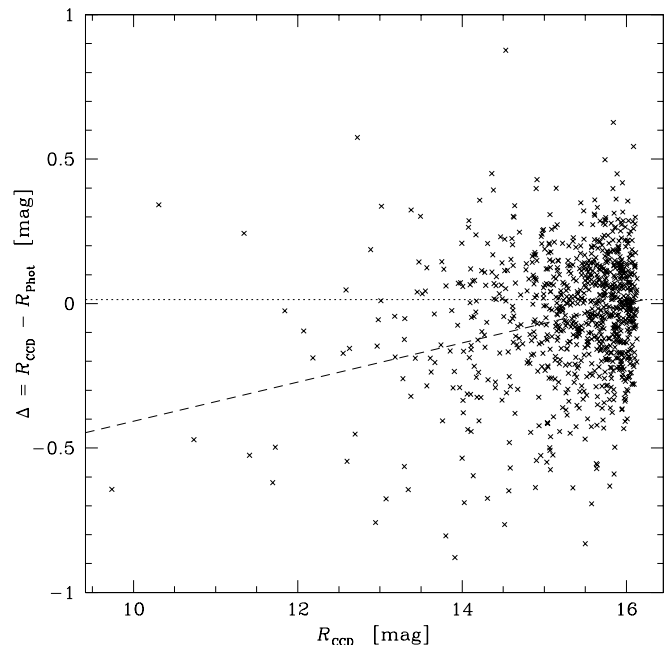


FIG. 2.—Comparison of  $R_{\text{ph}}$  with  $R_{\text{CCD}}$ . The dotted line shows the zero-point offset,  $\Delta = R_{\text{CCD}} - R_{\text{ph}} = 0.014 \pm 0.22$  mag. The dashed line shows the best-fit relation between  $\Delta$  and  $R_{\text{ph}}$ .

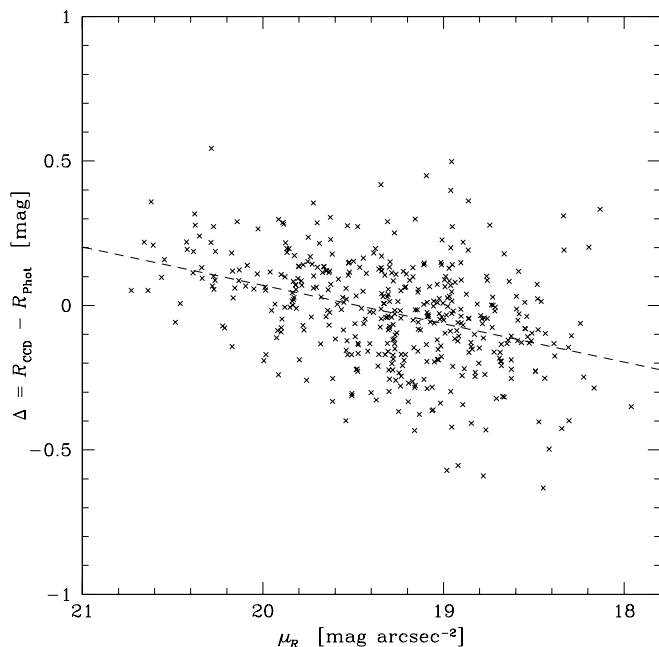


FIG. 3.— $\Delta$  as a function of peak surface brightness for 429 galaxies. The dashed line is the best fit.

Figure 4 shows  $\Delta$  as a function of  $(V-R)_{\text{CCD}}$  for the 508 galaxies in the same range of apparent magnitude as in Figure 3. The photographic magnitudes are too bright for the blue (generally low surface brightness) galaxies and too faint for the red (generally higher surface brightness) galaxies. The best-fit relation (dashed line) is  $\Delta = -0.66(V-R)_{\text{CCD}} + 0.36$ . Because central surface brightness and color are correlated, the underlying systematic effect is the same here as in Figure 3.

This correlation is shown in Figure 5, which is a plot of surface brightness,  $\mu_R$ , against color index  $(V-R)_{\text{CCD}}$  for the same sample of galaxies as in Figures 3 and 4.

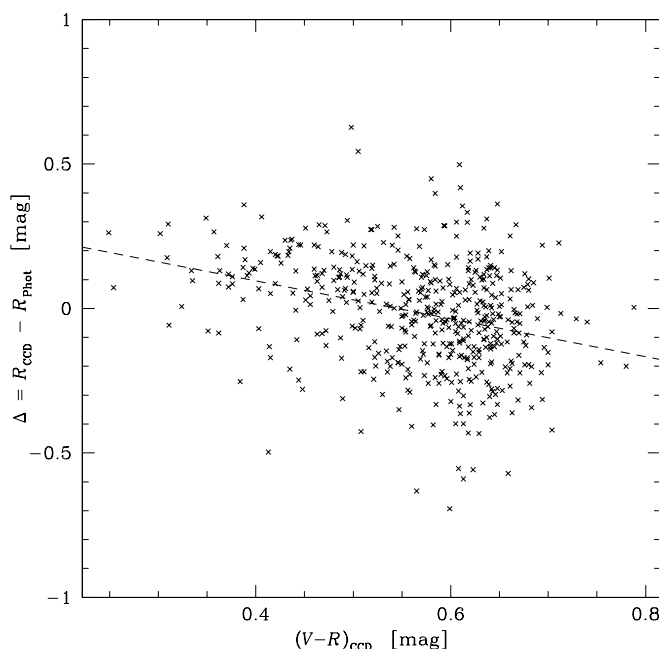


FIG. 4.— $\Delta$  as a function of color for 508 galaxies. The dashed line is the best-fit relation between  $\Delta$  and  $(V-R)_{\text{CCD}}$ .

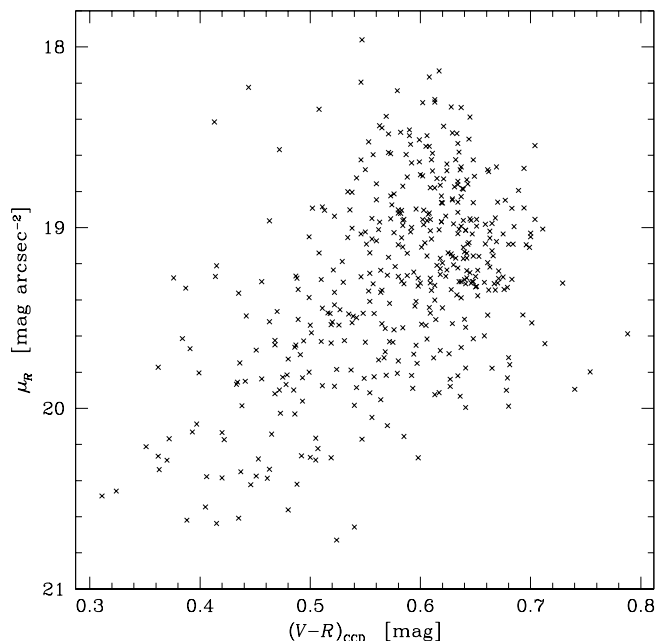


FIG. 5.—Surface brightness vs. color index for the galaxies in the OCS sample with  $15.5 < R < 16.13$  mag.

Table 1 lists the four magnitude-limited redshift surveys that can be extracted from the data in Tables 2 and 3 (along with the photometry from Table 3 of Brown et al. 2001) and their properties. In addition to the two samples, the OCS and DCS, originally derived from the plate scans, Brown et al. (2001) constructed two more rigorously defined magnitude-limited redshift surveys, the RCS and VCS, in the  $64 \text{ deg}^2$  region with CCD photometry. The uncorrected photographic photometry in Table 2 determines the limiting magnitude for the OCS and DCS surveys. Constructing samples from photometric surveys before correction for systematic effects has been standard procedure. However, as emphasized by Brown et al. (2001), making absorption and  $K$ -corrections before magnitude-limiting the sample ensures that the redshift survey samples galaxies of all spectroscopic types to the same effective depth. We derived the RCS and VSC samples *after* absorption- and  $K$ -correcting the relevant CCD magnitudes. Table 1 lists both the total number of galaxies in each sample and the number with redshifts; all the samples are more than 98% complete to the specified limit.

### 2.1. Morphological Types

One of us (G. A. W.) used a  $30\times$  magnifier to estimate morphological types for all OCS galaxies with photogra-

TABLE 1  
COMPLETE REDSHIFT SURVEYS IN THE CENTURY SURVEY REGION

Survey Name	R.A. Range (B1950.0) (hr)	Galaxies	Redshifts	Magnitude Limit
OCS ...	8.5–16.5	1754	1728	16.13 ( $R_{\text{ph}}$ )
DCS ...	8.53–10.75	508	507	16.4 ( $R_{\text{ph}}$ )
RCS ...	8.5–13.5	1274*	1251	16.2 ( $R_{\text{CCDe}}$ )
VCS ...	8.5–13.5	1279*	1255	16.7 ( $V_{\text{CCDe}}$ )

NOTE.—Total sample defined according to equation (2) of Brown et al. 2001.

TABLE 2  
PHOTOGRAPHIC CENTURY SURVEY

R.A. (1)	Decl. (2)	$R_{KC}$ (3)	$cz$ (4)	$cz$ Error <sup>a</sup> (5)	Type (6)	Note <sup>b</sup> (7)	Sample (8)	Note (9)
8 35 36.02.....	29 26 37.0	14.59	23,369	36	E		OCS	
8 35 49.07.....	28 53 13.0	15.50	15,458	71	Sc		OCS	Edge-on
8 35 54.24.....	29 25 38.2	16.16	23,836	58	...		DCS	
8 35 54.57.....	29 41 33.2	16.07	31,883	63	S0		OCS	
8 35 56.24.....	29 40 55.3	16.32	30,782	84	...		DCS	

NOTES.—Units of right ascension are hours, minutes, and seconds, and units of declination are degrees, arcminutes, and arcseconds. Table 2 is presented in its entirety in the electronic edition of the *Astronomical Journal*. A portion is shown here for guidance regarding its form and content.

<sup>a</sup> In this column, —1 denotes that an error is unavailable.

<sup>b</sup> (IP) Intersecting pair; (CG) companion galaxy; (NS) nearby star.

phic  $R_{ph} \leq 16.13$  from the glass copies of the POSS1 O (blue) plates, which for this work were found to be superior to the paper and digitized copies. With mounting distance, the classifications are increasingly difficult. At the largest redshifts, this amounts to an estimate of the disk-to-bulge ratios that can still be seen when spiral structure is no longer resolved. Consequently the Hubble types are in coarse bins: E, S0, Sa, Sb, Sc, and Irr plus the corresponding barred types. Double morphological type entries in Table 2 indicate galaxies with images on more than one plate; from these overlaps, we estimate that the classification error is  $\pm 1$  type.

For the region with CCD photometry, Figure 6 shows the  $(V-R)_{CCD}$  color distribution for each morphological type. We do not distinguish between barred and unbarred members of the class. From E through Sc, the mean color for each morphological type corresponds remarkably well to the colors quoted by Fukugita, Shimasaku, & Ichikawa (1995, hereafter FSI, Table 3a). Although sparsely populated, our color distribution for the Im/Irr class appears bimodal. The color of the blue peak corresponds to the typical  $V-R_C$  color (0.31) quoted by FSI. The CCD images reveal that many objects in the red “peak” are tight pairs: some of these show obvious tidal distortions and others are pairs of early-type galaxies. Most of these pairs are not clearly resolved on the POSS1 plates.

### 3. SPECTROSCOPIC OBSERVATIONS

Tables 2 and 3 list a total of 2437 galaxies in the CS region. All but 27 of the galaxies in Table 2 have redshifts; all but 14 redshifts were measured with Dartmouth or CfA facilities including the 2.4 m Hiltner telescope of the Michigan-Dartmouth-MIT (MDM) Observatory on Kitt

Peak, the Multiple Mirror Telescope (MMT) on Mount Hopkins, and the 1.5 m telescope of the Fred Lawrence Whipple Observatory.

We generally observed galaxies in the denser fields with the 2.4 m telescope using the Decaspec, a 10 object fiber instrument built for this project. We used the MMT (in its original configuration) and the Whipple Observatory 1.5 m to obtain individual spectra in more sparsely populated regions where the multiplexing feature of the Decaspec was not advantageous.

#### 3.1. MDM Decaspec Observations

We measured 1019 redshifts with the Decaspec or the Mark III Spectrograph on the 2.4 m Hiltner telescope at the MDM Observatory. Fabricant & Hertz (1990) describe the Decaspec, a fiber-moving head mounted on the telescope in front of the spectrograph. The Decaspec has 10 movable probes; each of the probes contains five  $2''$  diameter optical fibers set in a row with  $21''$  spacing. The probes run along parallel tracks over the  $20'$  diameter field of the 2.4 m Hiltner telescope. The motion of the probes along and perpendicular to the tracks combined with instrument rotation enables target acquisition with one fiber per probe. The light from the Decaspec feeds into the Mark III spectrograph, designed by W. A. Hiltner.

We made all the CS observations with a  $300 \text{ line mm}^{-1}$  grism blazed at  $5400 \text{ \AA}$ . The Decaspec observations began in 1989 May. We used a number of CCD detectors during the course of the observations. All these detectors delivered a resolution of  $\sim 12 \text{ \AA}$  FWHM and a spectral coverage of approximately  $4000\text{--}7000 \text{ \AA}$ .

The observations usually consisted of three 40 minute integrations to enable cosmic-ray rejection. Our subsequent data reductions to one-dimensional spectra used the APEXTRACT package in IRAF<sup>3</sup> (Tody 1986). We used standard data reduction techniques with custom scripts written to simplify the bookkeeping. We used the IMCOMBINE option to combine the three spectra and extracted the resulting spectrum with APSUM. We used continuum spectra from a screen inside the dome for flattening; we constructed individual wavelength calibrations from HgNeXe comparison exposures before and after each object integration. Generally we fitted a fourth- or fifth-order poly-

TABLE 3

VELOCITIES OBTAINED FOR THE RCS AND VCS SAMPLES

R.A. (J2000.0) (1)	Decl. (J2000.0) (3)	$cz$ (3)	$cz$ Error (4)
8 36 05.38.....	28 49 28.9	15,454	37
8 36 20.77.....	29 16 37.6	23,056	31
8 36 56.09.....	29 48 06.4	15,042	32
8 37 12.46.....	29 43 44.7	31,879	33
8 37 21.34.....	29 35 42.9	14,323	29
8 38 14.95.....	29 45 20.6	32,578	30

NOTES.—Table 3 is presented in its entirety in the electronic edition of the *Astronomical Journal*. A portion is shown here for guidance regarding its form and content.

<sup>3</sup> IRAF is distributed by the National Optical Astronomy Observatory, which is operated by the Association of Universities for Research in Astronomy, Inc., under contract with the National Science Foundation.

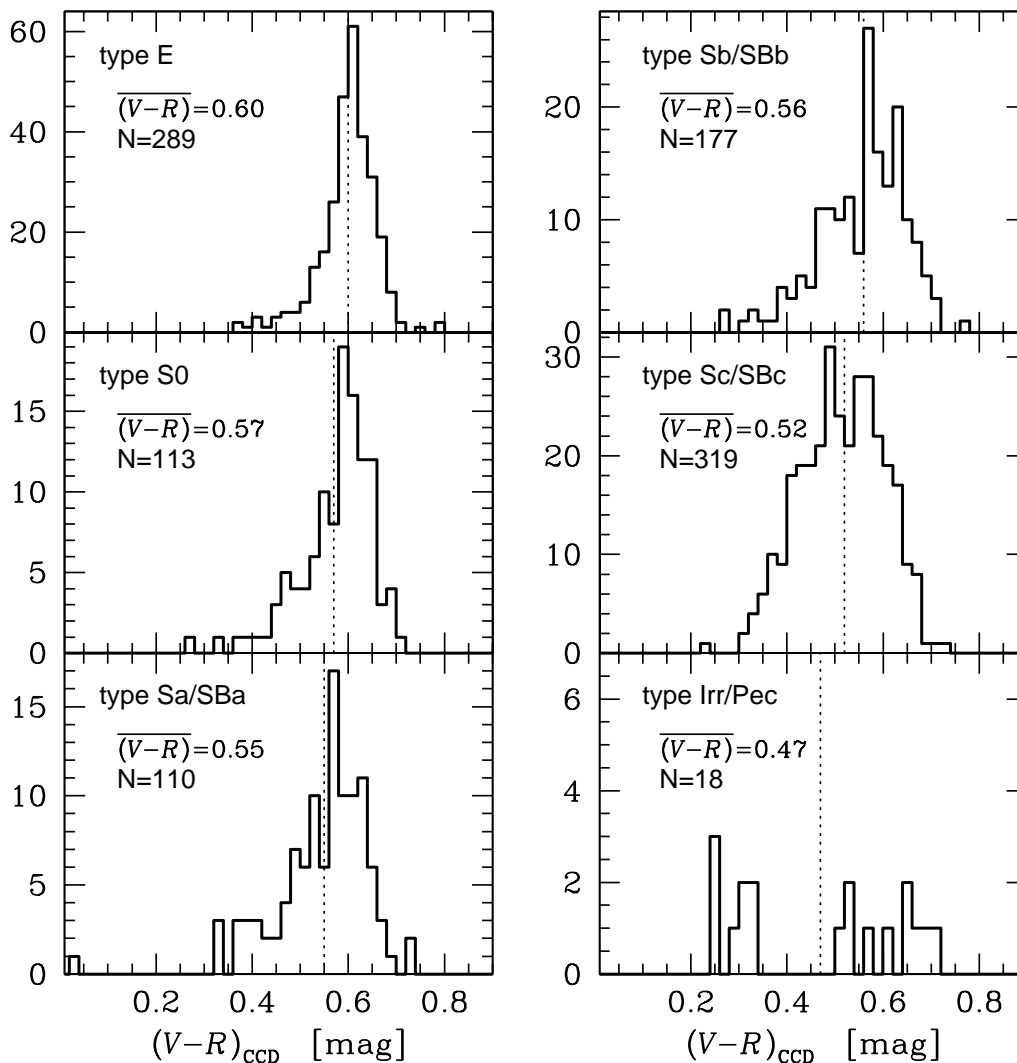


FIG. 6.— $(V-R)_{\text{CCD}}$  color distributions for each morphological type. Each panel gives the mean color and the number of galaxies,  $N$ .

nomial to the nonlinear part of the wavelength correction curve.

We used the four nonobject fibers from each probe of the Decaspec for sky subtraction. We corrected differences in the fiber transmission by normalizing the strong  $\lambda 5577$  night-sky line equivalent widths in all the spectra to the galaxy fiber and then subtracting the median of the four spectra from the object spectrum. By dividing the galaxy spectra by very high signal-to-noise ratio blue-star spectra (with all stellar absorption lines removed) normalized to 1.0 everywhere, we eliminated the strong telluric night-sky absorptions in the red due to water and  $\text{O}_2$ .

To produce template spectra, we observed velocity standards at least once nightly. The templates included stars used routinely at the CfA along with IAU radial velocity standards from the Astronomical Almanac. We obtained at least 10 separate spectra through one fiber in each of the 10 probes. We reduced these spectra as described above; we then removed velocity shifts and summed the spectra to produce a template.

Thorstensen (Thorstensen et al. 1989) wrote the software to extract redshifts and their estimated errors. The software

includes the Tonry & Davis (1979) cross-correlation algorithm for absorption-line spectra and a multiple Gaussian-fitting routine for emission lines. We accepted only cross-correlation velocities with high formal statistical confidence; we checked all fits by eye. For most objects,  $R \geq 3.0$  with  $R > 10$  common. The mean uncertainty in redshifts derived from the Decaspec is  $\pm 44.5 \text{ km s}^{-1}$ .

We observed several hundred galaxies one by one with the Mark III spectrograph or the 1.5 FWLO spectrograph. The data reductions were identical to those in the redshift survey of the fainter Zwicky galaxies in the first CfA strip (Thorstensen et al. 1989, 1995; Wegner et al. 1990).

### 3.2. MMT Observations

We observed 1079 galaxies with the Multiple Mirror Telescope (MMT). We used the blue channel of the MMT spectrograph and the photon-counting Reticon system (Latham 1982) and, later, the blue and red channels with CCD detectors for the observations. The reduction to heliocentric radial velocity employed the RVSAO package of Kurtz et al. (1992) and Mink & Wyatt (1992) was developed at the CfA and closely resembles the MDM procedures.

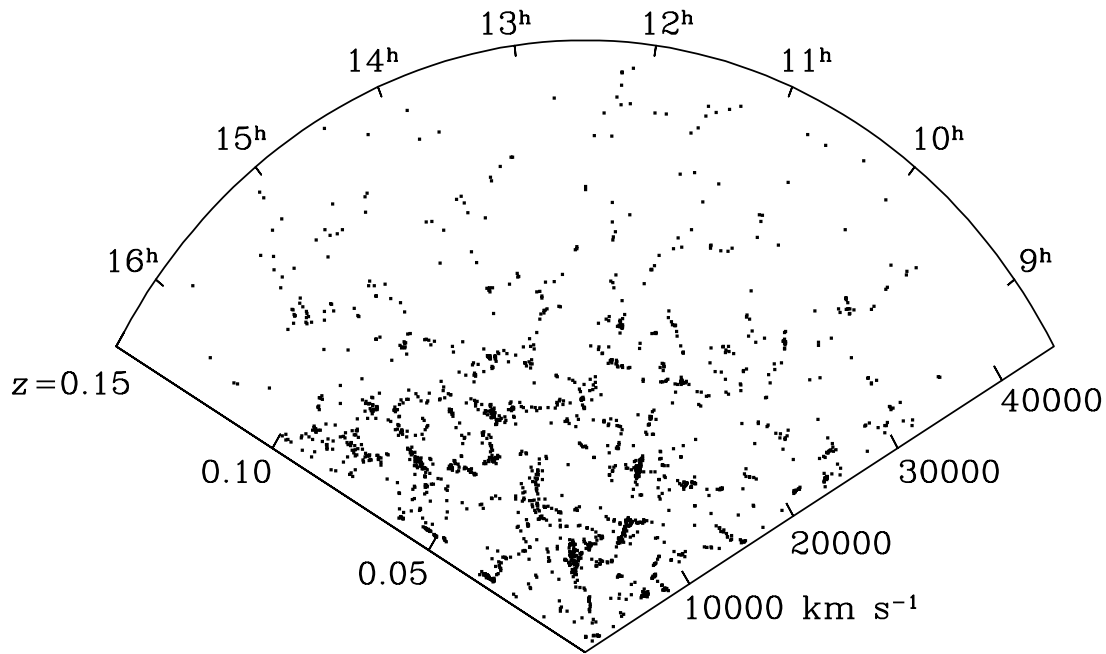


FIG. 7.—Cone diagram for the OCS for  $z \leq 0.15$ . For clarity, we omit galaxies with  $cz \leq 1000 \text{ km s}^{-1}$ .

These techniques are described by Huchra, Geller, & Corwin (1995) and Huchra, Vogele, & Geller (1999). The typical external error in the MMT velocities is  $\sim 35 \text{ km s}^{-1}$ .

### 3.3. Recent 1.5 m FLWO Observations

To complete the RCS and VCS (Brown et al. 2001), we measured 226 new redshifts with the FAST (Fabricant et al. 1998) spectrograph on the Fred Lawrence Whipple Observatory 1.5 m telescope in 2000 April and 2000 November; Table 3 lists these redshifts. From 1994 through 1996, we

also used FAST to measure 72 redshifts in the OCS (included in Table 2). We used the 300 line  $\text{mm}^{-1}$  grating with  $6 \text{ \AA}$  resolution and measured velocities with the cross-correlation package RVSAO (Kurtz & Mink 1998). The mean uncertainty of the velocities is  $\pm 40 \text{ km s}^{-1}$ .

### 3.4. Previously Published Redshifts

Some of our redshifts have been published previously: 164 redshifts are from Huchra et al. (1990), 92 are from Thorstensen et al. (1989), and 11 are from Willmer et al.

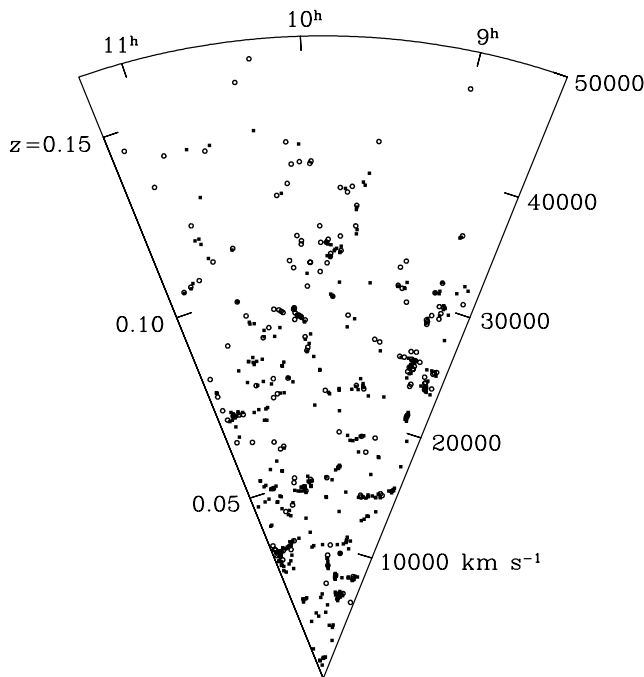


FIG. 8.—Cone diagram for the DCS. Squares represent galaxies in the OCS with  $R_{\text{ph}} \leq 16.13$ . Circles represent galaxies with  $16.13 < R_{\text{ph}} \leq 16.4$ . The redshift limits are the same as in Fig. 6.

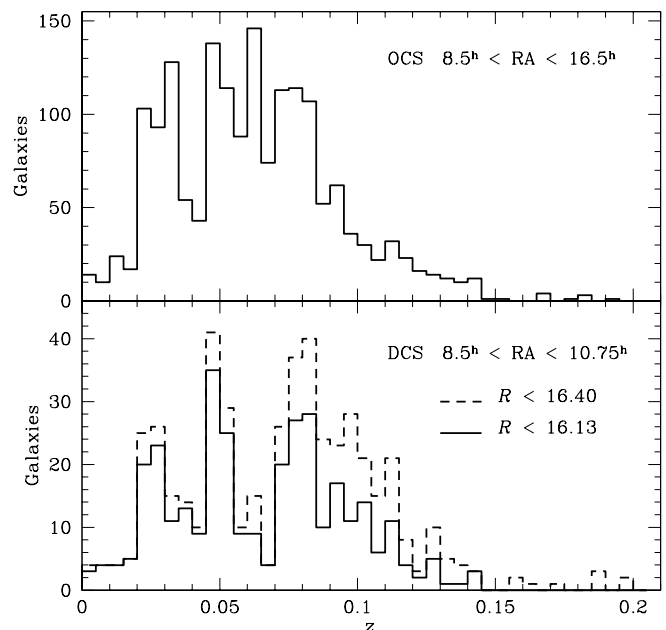


FIG. 9.—Redshift histograms for the OCS (top) and the DCS (bottom). In the DCS, the solid histogram refers to the galaxies also in the OCS; the dashed histogram refers to galaxies with  $R_{\text{ph}} \leq 16.4$ .

(1996). The Huchra et al. (1990) and Thorstensen et al. (1989) redshifts were acquired using the same instruments and reduction methods described above; they have the same zero points and errors.

#### 4. CATALOG OF REDSHIFTS

Table 2 lists the data for the OCS, for the DCS, and for some fainter objects. Columns (1) and (2) list the epoch J2000.0 right ascension and declination measured from the POSS1 plates (these coordinates agree very well with the ones determined from the CCD images). Column (3) lists the  $R_{\text{ph}}$  magnitude calibrated as in Geller et al. (1997) and as described in § 2.

Columns (4) and (5) contain the heliocentric redshift and its error, respectively. Column (6) lists the estimated morphological type. Column (7) contains notes for objects with poor positions: IP indicates an interacting galaxy pair, CG indicates a companion galaxy, and NS indicates a nearby star. Column (8) contains the sample designation (OCS or DCS). Column (9) contains G. A. W.'s classification notes.

For galaxies required to complete the samples of Brown et al (2001), Table 3 lists epoch J2000.0 right ascension and declination (cols. [1] and [2], respectively), columns (3) and (4) are the heliocentric redshift and its error, respectively. Brown et al. (2001; Table 3) publish CCD  $V$  and  $R_{\text{KC}}$  magnitudes, galactic extinctions, and  $K$ -terms for *all* of the galaxies in their samples.

The cone diagrams in Figures 7 and 8 show the two complete redshift surveys defined from the photographic photometry in Table 2. Figure 9 shows the corresponding redshift histograms. The Great Wall contributes the peak at redshifts between 0.02 and 0.035.

Geller et al. (1997) discuss the OCS; they derive an  $R$ -band luminosity function and luminosity density  $j = (2.8 \pm 0.9) \times 10^8 L_{\odot}$ , in excellent agreement with the value recently reported by Blanton et al. (2001), who analyze a portion of the Sloan Digital Sky Survey. Brown et al. (2001) derive an  $R$ -band luminosity function and corresponding luminosity density for the CCD-based RCS. Their results are consistent with the photographic determination. Brown et al. show further that the OCS omits few low surface brightness (LSB) galaxies with  $\mu(0)_R > 20.8$  mag arcsec $^{-2}$ ; the photographic catalog contains 12 LSB galaxies with  $R_{\text{ph}} < 16.13$ , and the CCD catalog contains 15 in the overlap region.

The DCS in Figure 8 is 0.27 mag deeper than the OCS over the right ascension range  $8^{\text{h}}5 \leq \alpha \leq 13^{\text{h}}5$ , equinox B1950.0. There are 518 galaxies in this sample; 177 of them have  $R_{\text{ph}} > 16.13$ . Generally, the fainter galaxies (*circles*) populate structures already defined by the brighter sample

(*squares*). The histogram in Figure 9 (*bottom*) shows the redshift distribution for the  $R_{\text{ph}} < 16.13$  galaxies and for the fainter sample. It is again apparent that both sets of galaxies trace the same structures; the distribution of the fainter sample shifts toward larger redshift as expected.

#### 5. CONCLUSIONS

The 2410 redshifts we report here constitute four complete redshift surveys in the Century Survey region. We include photographic photometry and morphological types for most of the galaxies.

Papers in the literature discuss three of the surveys: the OCS, the RCS, and the VCS. Brown et al. (2001) tabulate the  $V$  and  $R$  CCD photometry for the RCS and VCS. They also list absorption and  $K$ -corrections for the samples.

The DCS appears only in this paper. Not surprisingly, the fainter galaxies in the DCS populate features defined by the original Century Survey in the region.

Redshifts in the Century Survey region are useful for the analysis and interpretation of other surveys. For example, the depth of the OCS, RCS, and VCS is comparable with the depth of the 2MASS  $J$ -band survey (Jarrett et al. 2000) and should provide a sizable magnitude-limited sample for computation of the  $J$ -band luminosity function and for some assessment of its morphological type dependence.

The surveys we discuss also cover 90% of the KPNO International Spectroscopic Survey (KISS) region (Salzer et al. 2000). KISS is an objective-prism survey. Availability of the CS data enables comparison of the distribution of the KISS sample galaxies with those in a complete magnitude-limited redshift survey.

We thank Tim Beers for suggesting the name "Century Survey." We are grateful to Bill van Altena for making the Yale PDS available to us and for making our many plate-scanning visits to Yale pleasant. The Yale PDS facility was supported by NSF. At Dartmouth, this project was partially funded from Dartmouth College and by two funding agencies. J. R. T. was supported in part by NSF grant AST 86-20081 and a Research Corporation Cottrell Grant. G. W. was supported in part by NSF grants AST 86-20081, AST 90-23450, and AST 93-47714. We thank the MDM Observatory staff, especially Bob Barr, for excellent support at the 2.4 m telescope. The Smithsonian Institution funded this project at the CfA. We thank Emilio Falco and Rudy Schild for making some of the photometric observations we used to calibrate the photographic photometry. The MMT night assistants, Carol Heller, John McAfee, and Janet Miller, provided invaluable support, and Suzan Tokarz helped with data reductions.

#### REFERENCES

- Bertin, E., & Arnouts, S. 1996, A&AS, 117, 393  
 Blanton, M. R., et al. 2001, AJ, 121, 2358  
 Brown, W. R., Geller, M. J., Fabricant, D. G., & Kurtz, M. J. 2001, AJ, 122, 714  
 Cross, N., et al. 2001, MNRAS, 324, 825  
 da Costa, L. N., et al. 1994, ApJ, 424, L1  
 Davis, M., Huchra, J. P., Latham, D. W., & Tonry, J. 1982, ApJ, 253, 423  
 Fabricant, D., Cheimets, P., Caldwell, N., & Geary, J. 1998, PASP, 110, 79  
 Fabricant, D., & Hertz, E. 1990, Proc. SPIE, 1235, 747  
 Fukugita, M., Shimasaku, K., & Ichikawa, T. 1995, PASP, 107, 945 (FSI)  
 Geller, M. J., & Huchra, J. P. 1989, Science, 246, 897  
 Geller, M. J., et al. 1997, AJ, 114, 2205  
 Giovanelli, R., & Haynes, M. P. 1989, AJ, 97, 633  
 Huchra, J. P., Geller, M. J., & Corwin, H. G., Jr. 1995, ApJS, 99, 391  
 Huchra, J. P., Geller, M. J., de Lapparent, V., & Corwin, H. G., Jr. 1990, ApJS, 72, 433  
 Huchra, J. P., Vogeley, M. S., & Geller, M. J. 1999, ApJS, 121, 287  
 Jarrett, T. H., Chester, T., Cutri, R., Schneider, S., Skrutskie, M., & Huchra, J. P. 2000, AJ, 119, 2498  
 Kent, S. M., Ramella, M., & Nonino, M. 1993, AJ, 105, 393  
 Kron, G. E., White, H. S., & Gascoigne, S. C. B. 1953, ApJ, 118, 502  
 Kurtz, M. J., Huchra, J. P., Beers, T. C., Geller, M. J., Gioia, I. M., Maccararo, T., Schild, R. E., & Stauffer, J. R. 1985, AJ, 90, 1665  
 Kurtz, M., & Mink, D. 1998, PASP, 110, 934  
 Kurtz, M. J., Mink, D. J., Wyatt, W. F., Fabricant, D. G., Torres, G., Kriss, G. A., & Tonry, J. L. 1992, in ASP Conf. Ser. 25, Astronomical Data Analysis, Software and Systems I, ed. D. M. Worrall, C. Biemesderfer, & J. Barnes (San Francisco: ASP), 432  
 Latham, D. 1982, in Instrumentation for Astronomy with Large Optical Telescopes, ed. C. M. Humphries (Dordrecht: Reidel) 259  
 Loveday, J., Peterson, B. A., Efstathiou, G., & Maddox, S. J. 1992, ApJ, 390, 338

- Mink, D. J., & Wyatt, W. F. 1992, in ASP Conf. Ser. 25, *Astronomical Data Analysis, Software and Systems I*, ed. D. M. Worrall, C. Biemesderfer, & J. Barnes (San Francisco: ASP), 439
- Ramella, M., Nonino, M., & Geller, M. J. 1995, *Mem. Soc. Astron. Italiana*, 66, 113
- Ratcliffe, A., Shanks, T., Broadbent, A., Parker, Q. A., Watson, F. G., Oates, A. P., Fong, R., & Collins, C. A. 1996, *MNRAS*, 281, L47
- Salzer, J. J., et al. 2000, *AJ*, 120, 80
- Shectman, S. A., Landy, S. D., Oemler, A., Tucker, D. L., Lin, H., Kirshner, R. P., & Schechter, P. L. 1996, *ApJ*, 470, 172
- Thorstensen, J. R., Kurtz, M. J., Geller, M. J., Ringwald, F. A., & Wegner, G. 1995, *AJ*, 109, 2368
- Thorstensen, J. R., Wegner, G. A., Hamwey, R., Boley, F., Geller, M. J., Juchra, J. P., Kurtz, M. J., & McMahan, R. K. 1989, *AJ*, 98, 1143
- Tody, D. 1986, *Proc. SPIE*, 627, 733
- Tonry, J., & Davis, M. 1979, *AJ*, 84, 1511
- Vettolani, G., et al. 1997, *A&A*, 325, 954
- Wegner, G., Thorstensen, J. R., Kurtz, M. J., Geller, M. J., & Huchra, J. P. 1990, *AJ*, 100, 1405
- Willmer, C. N. A., Koo, D. C., Ellman, N., Kurtz, M. J., & Szalay, A. S. 1996, *ApJS*, 104, 199
- York, D. G., et al. 2000, *AJ*, 120, 1579